

Growth Deceleration of Vertically Aligned Carbon Nanotube Arrays: Catalyst Deactivation or Feedstock Diffusion Controlled?

Rong Xiang,^{†,‡} Zhou Yang,[‡] Qiang Zhang,[‡] Guohua Luo,[‡] Weizhong Qian,[‡] Fei Wei,^{*,‡} Masayuki Kadowaki,[†] Erik Einarsson,[†] and Shigeo Maruyama^{*,†}

Department of Mechanical Engineering, The University of Tokyo, 7-3-1 Hongo, Bunkyo-ku, Tokyo 113-8656, Japan, and Beijing Key Laboratory of Green Chemical Reaction Engineering and Technology, Department of Chemical Engineering, Tsinghua University, Beijing 100084, China

Received: November 9, 2007; In Final Form: December 22, 2007

Feedstock and byproduct diffusion in the root growth of aligned carbon nanotube arrays is discussed. A non-dimensional modulus is proposed to differentiate catalyst-poisoning controlled growth deceleration from one which is diffusion controlled. It is found that, at the current stage, aligned multiwalled carbon nanotube arrays are usually free of feedstock diffusion resistance while single-walled carbon nanotube arrays are already suffering from a strong diffusion resistance. The method presented here is also able to predict the critical lengths in different CVD processes from which carbon nanotube arrays begin to meet strong diffusion resistance, as well as the possible solutions to this diffusion caused growth deceleration.

Vertically aligned carbon nanotube (CNT) arrays grown on flat substrates,^{1–7} in which all the nanotubes are of similar orientation and length, offer an ideal platform to study CNT growth mechanisms and kinetics. Since 1996,¹ various chemical vapor deposition (CVD) methods, including floating catalytic CVD,² plasma enhanced CVD,³ and thermal CVD⁴ have been proposed to synthesize aligned multiwalled carbon nanotube (MWNT) arrays. Lately, alcohol catalytic CVD⁵ (ACCVD), water assisted CVD,⁶ microwave plasma CVD,⁷ and so forth are used to produce vertically aligned single-walled carbon nanotube (SWNT) arrays. These processes usually involve different catalysts, carbon sources, and operation parameters, resulting in products with different morphologies and qualities. However, none of these CNT growth processes can overcome the gradual deceleration and eventual termination of growth. The ability to understand and thereby to overcome the underlying deactivation mechanisms becomes one of the most critical steps to develop nanoscale tubes into real macroscopic materials.

Many groups have affirmed the root growth mode of their vertically aligned CNTs, indicating that the feedstock molecules have to diffuse through the thick CNT array, reach the substrate where catalysts are located, and then contribute to the CNT growth.^{8–13} In this bottom-up growth process, the diffusion resistance of the feedstock from the top to the root arises as an obstruction and can act as a unique decelerating growth mechanism. Existence of a feedstock diffusion resistance means that concentration of the carbon source at the CNT root should be lower than the bulk concentration. Previously, Zhu et al.¹⁴ fitted experimentally obtained film thicknesses with the square root of growth time and stated that the growth deceleration is attributed to the strong diffusion limit of feedstock to the CNT root. However, Hart et al.¹⁵ claimed later that their growth curve can be accurately described by either diffusion limit or catalyst

deactivation, suggesting that only fitting is not sufficient to clarify a diffusion controlled process from a catalyst deactivation controlled one. Furthermore, if the process is in the transition region, that is, not completely diffusion controlled, root square fitting is no longer available. Here, we propose a method of using a nondimensional modulus to quantitatively evaluate the degree of feedstock diffusion resistance (no diffusion resistance regime, transient regime, and strong diffusion limit regime). ACCVD¹⁶ grown single-walled carbon nanotubes (SWNTs)^{5,17–20} were used as a typical example of this method and were found to be essentially free of feedstock diffusion resistance. The byproduct back diffusion,¹⁹ which has never been taken into account previously, can also be estimated by the present method. Considering the similar diffusion behavior in different CVD processes, five of the most frequently used systems are also discussed. The results agree well with the currently available experimental results.

Vertically aligned SWNTs were synthesized on Co/Mo dip-coated²¹ quartz substrates at 800 °C from ethanol as a carbon source. MWNT arrays were grown on quartz substrates at 800 °C with simultaneous feeding of cyclohexane and ferrocene.²² Details of the growth processes can be found in our previous work.^{17,22} The lengths of as-grown CNT arrays were measured by SEM (JSM-7000 and JSM-7401), and average diameters were determined by TEM (JOEL 2010).

First, it is worth clarifying the concept of diffusion limit that is to be discussed below. Figure 1 presents the root growth process of aligned CNT arrays. A carbon source is being decomposed and extruded into solid CNT on catalyst. The concentration of feedstock molecules (e.g., ethanol in ACCVD) at the CNT root, which chemically determined the reaction rate, will be much lower than top (bulk concentration) if feedstock molecules are not diffusing fast enough from top to root. Similarly, if the byproduct molecules generated by CNT growth cannot diffuse fast, their concentration will also be higher at CNT root than near the top. This concentration difference between the root and top of a CNT array is the origin of diffusion limit. Other facts, such as catalyst oxidation, aggrega-

* To whom correspondence should be addressed. E-mail: weifei@flou.org. Phone: 86-10-62788984. Fax: 86-10-62772051 (F.W.). E-mail: maruyama@photon.t.u-tokyo.ac.jp. Phone: 81-3-5841-6421. Fax: 81-3-5800-6983 (S.M.).

[†] The University of Tokyo.

[‡] Tsinghua University.

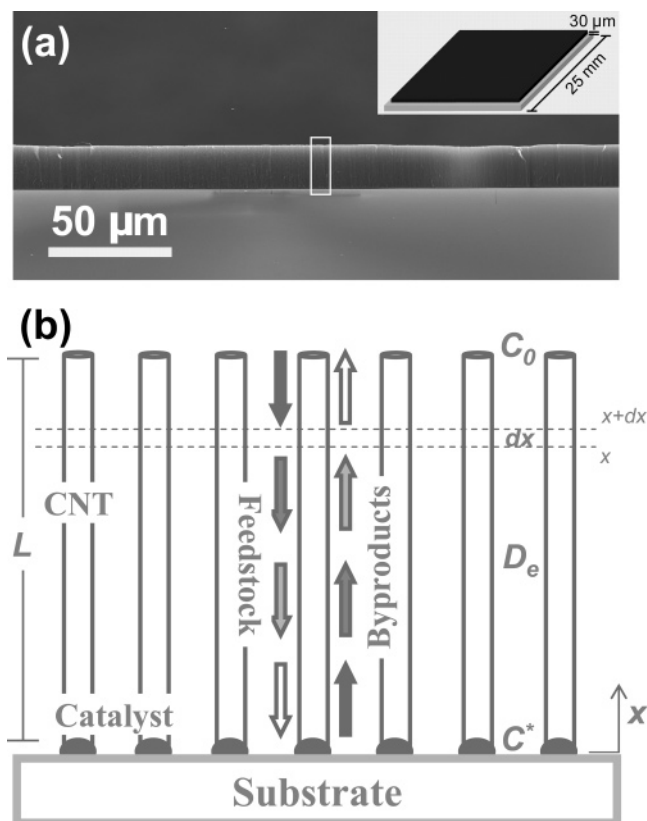


Figure 1. (a) SEM micrograph of vertically aligned SWNT arrays from ACCVD, inset at top-right is a schematic of a CNT film on substrate, suggesting the different dimensions of film size and thickness; (b) schematic presentation describing the diffusion of feedstock as well as gas product during the root growth of CNT arrays.

tion, reaction with substrate, formation of amorphous soot, or graphitic structure covered on catalyst particles, are attributed to the catalyst poisoning (causing smaller k_s as to be discussed later), although some of them, for example, soot formation, also prohibit carbon source from reaching catalyst. Also, we only consider one-dimensional diffusion (along the tube axis) inside the CNT array. The diffusion from the sides of the forest is neglected because of the following two reasons. First, the side diffusion distance, that is, the width of the vertically aligned CNT film (~ 25 mm) is usually much larger than the top diffusion distance, that is, the film thickness (usually several millimeters at most). Second, side diffusion is probably more difficult because of the higher collision frequency in the anisotropic structure of the vertically aligned CNT array. Therefore, in a small sliced CNT array region dx (as indicated by dashed lines in Figure 1b), the difference in the amount of feedstock diffusing in from the top and diffusing out from the bottom should be what is consumed inside this dx region. At CNT–substrate interface, although microscopically (at molecular level) not all collisions between feedstock molecule and catalyst can result in CNT growth, the macroscopic net diffusion flux equals to the CNT formation rate (either expressed by the reaction rate $k_s SC^{*m}$ or the macroscopic growth rate $aSdL/dt$) when in equilibrium. Following basic diffusion theory (Fick’s Law, diffusion flux is proportional to concentration gradient) and reaction theory,²³ this process can be expressed by

$$D_e S \left(\frac{dC}{dx} \right)_{x+dx} - D_e S \left(\frac{dC}{dx} \right)_x = 0 \quad (\text{inside of CNT forest}) \quad (1)$$

and

$$D_e S \left(\frac{dC}{dx} \right)_{x=0} = k_s SC^{*m} = aS \frac{dL}{dt} \quad (\text{root of CNT forest}) \quad (2)$$

where D_e is the effective diffusion coefficient, S film area, x normal coordinate from substrate, L length of CNT array, k_s surface reaction constant of carbon source to CNT, C^* effective feedstock concentration at the CNT root, m reaction order, and a structure-dependent constant of CNT array. Here, we emphasize that, although CNT growth can be divided into detailed steps, that is, first feedstock decomposition, then carbon diffusion inside metal, and final carbon precipitation, all of these steps are treated as if they were together here and k_s is the reaction constant of the overall process from carbon source to CNTs. In other words, k_s represents the dependence of overall CNT growth rate on carbon source concentration. This is also the only growth constant that we can obtain directly from experiments. Equation 1 is solved as $d^2C/dx^2 = 0$ or $dC/dx = \text{constant}$ and means that the feedstock concentration is linearly decreasing from top to root; thus, eq 2 can be modified to

$$D_e S \frac{C_0 - C^*}{L} = k_s SC^{*m} = aS \frac{dL}{dt} \quad (3)$$

Therefore, as soon as we know the reaction order m and the reaction coefficient k_s , the effective concentration C^* can be found from eq 3 and then the time-dependent growth curve can be determined from an integration of eq 3.

Experiments were carried out under different ethanol pressures to investigate the growth order in the ACCVD method. It is found that the initial growth rate is almost proportional to the ethanol concentration²⁰ (see Supporting Information), suggesting $m = 1$, which is also found to be approximately valid in other processes (e.g., for water assisted super growth²⁴). If k_s can be constant, the effective concentration C^* is calculated as $C^* = D_e C_0 / (D_e + Lk_s)$. Then, eq 3 becomes

$$a \frac{dL}{dt} = k_s C^* = k_s \frac{D_e C_0}{D_e + Lk_s} \quad (4)$$

By integrating eq 4, time-dependent growth curve is deduced as

$$L = \sqrt{\left(\frac{D_e}{k_s} \right)^2 + \frac{2D_e C_0}{a} t} - \frac{D_e}{k_s} \quad (5)$$

This equation can be proportional to either t (no diffusion limit) or $t^{1/2}$ (strong diffusion limit), depending on the values of $2D_e C_0 t/a$ and D_e/k_s (see Supporting Information). It is similar to what is widely used in silicon oxidation, the so-called “Deal-Grove” relationship,²⁵ as discussed previously.^{14,26} One can, in principle, also predict the growth curve of a CNT array provided that all of the parameters listed above are known. However, a big difference between growth of a CNT array and silicon oxide is that, in most cases, the catalyst for CNT growth undergoes catalyst poisoning. Therefore, k_s in CNT growth is also a time-dependent parameter, unlike in silicon oxidation, where k_s is constant. This means that eq 5 only predicts the ideal growth curve where catalyst activity does not decay.

To enable a simple estimate on the existence of a diffusion limit for a certain system and CNT length, we can define a nondimensional number φ by

$$\varphi = \frac{k_s L}{D_e} \quad (6)$$

This number represents physically the ratio of catalytic capability to diffusive capability. Then, the ratio of effective concentration to bulk concentration, η (usually called the effective factor) can be correlated with φ via a simple function from eq 4 as

$$\eta = \frac{C^*}{C_0} = \frac{D_e}{k_s L + D_e} = \frac{1}{\varphi + 1} \quad (7)$$

This factor allows us to quantitatively characterize the degree of the diffusion limit. When φ is small (e.g., <0.1), it is much easier to diffuse than to react; thus, the effective factor will be nearly 1 ($\eta > 0.9$), indicating there is little diffusion resistance. In contrast, when φ is large (e.g., >9), it is more difficult to diffuse than to react; thus, the effective factor η will be nearly zero (<0.1) and the overall reaction will be dominated by the diffusion rate. The in-between situation is what we mentioned before as the transition regime, where the growth curve will be proportional to neither t nor $t^{1/2}$.

In ACCVD synthesis, the carbon feedstock at top of the SWNT array is constantly refreshed, and therefore the byproduct concentration can be treated as zero due to the high ethanol flow rate. Thus, if we assume that one C_2H_5OH molecule produces one byproduct molecule, for example, H_2O or H_2 , after decomposition ($A \rightarrow CNT + B + \dots$), the byproduct concentration at the CNT root can be also revealed as a single function of φ ,

$$C_B^* = C_0 \times \sqrt{\frac{M_B}{M_A}} \times \left(\frac{\varphi}{\varphi + 1} \right) \quad (8)$$

According to the above discussion, as long as we know D_e and k_s , the influence of diffusion can be concluded simply from the value of φ for a certain CNT length L . We know that the average diameter of SWNTs produced by ACCVD is about 2 nm, and the density of the as-grown film is about 0.04 g/cm^3 . Therefore, the average distance between adjacent SWNTs can be easily calculated to be 8.8 nm. As the mean free path of ethanol in this process is about 16000 nm, much larger than the distance between SWNTs, it can be concluded that the ethanol diffusion resistance is mainly due to the ethanol–CNT

collisions, that is, in the range of Knudsen diffusion. Thereby, the diffusion coefficient can be estimated from collision theory if assuming CNT tortuosity as diffusion channel tortuosity.²⁷ As for k_s , we can use the initial value at $t = 0$ when the CNT growth is free of diffusion resistance. With the estimated D_e and experiment-derived k_s , φ is calculated to be 0.054 ($\ll 1$) for $30 \mu\text{m}$ SWNT arrays in ACCVD. This means the ethanol concentration at the CNT root, where the catalyst is located, is almost the same as the concentration at the CNT top (95% from eq 7). The vertical distribution of ethanol concentration in the array is plotted in Figure 2a as A-SWNT. Thus, this process is catalyst deactivation controlled rather than diffusion controlled. After we peel the as-grown film off the substrate, most of the catalysts remain on the substrate, but the substrate is not active for a second growth. This confirmed that the catalyst poisoning contributed to the growth deceleration, which agrees with above calculation of φ . We know H_2O is a byproduct of ethanol decomposition; estimating through eq 8 reveals the concentration of water at the CNT root is several hundred parts per million. Considering the previous report on the critical role of H_2O or O_2 on the growth of SWNT,^{6,16,28} we plot the concentration distribution of H_2O in Figure 2a. This result is interesting, but currently we are not sure if this water concentration is critical for successful SWNT nucleation or its relation to catalyst deactivation in ACCVD. Further work is needed in this area.

One may notice that the above discussion on the feedstock diffusion is versatile and valid for all of the first-order growth methods of aligned CNTs, applying to both SWNTs and MWNTs. Therefore, with the available data in the literature, we are able to estimate the degree of diffusion resistance in other CVD processes used to grow aligned CNT forests. The only difference here is, when estimating the effective diffusion coefficient for MWNT arrays, the molecular diffusion should also be taken into account because the mean free path is comparable to the intertube distance for MWNT arrays, as listed in Table 1.

We analyzed four other CVD processes: a 2 mm MWNT array by floating CVD^{22,29–31} (F–MWNT), a 2.5 mm SWNT array by super growth by Hata et al.^{6,24,32} (S–SWNT), a 2.5 mm SWNT array by microwave plasma CVD by Zhong et al.^{7,26,33} (P–SWNT), and a 400 μm MWNT by thermal CVD by Zhu et al.^{11,14,34} (T–MWNT). The results are compared with our $30 \mu\text{m}$ SWNT array produced by ACCVD (A–SWNT) in Table 1. It can be seen that, k_s and D_e , the two key parameters

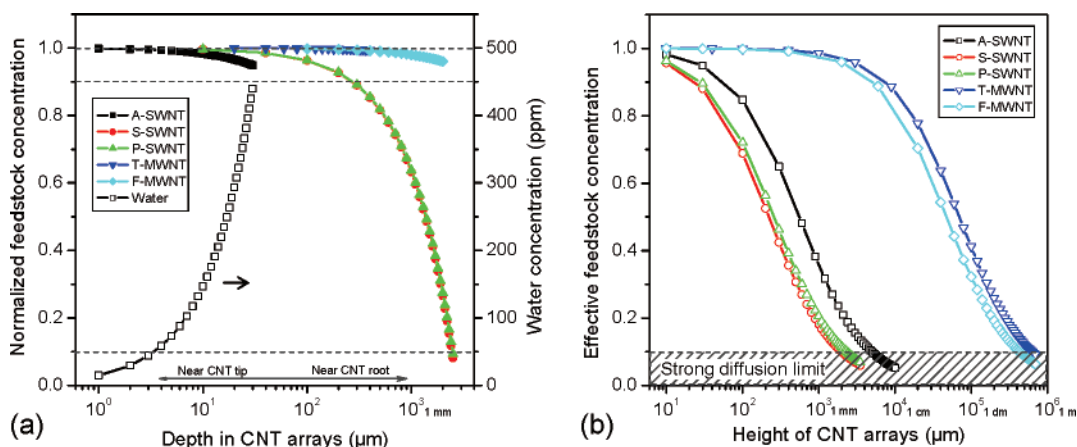


Figure 2. (a) Carbon source and byproduct concentration distribution in various vertically aligned CNT arrays. A-SWNT, $30 \mu\text{m}$ SWNT from ACCVD; S-SWNT, 2.5 mm SWNT from water-assisted super growth; P-SWNT, 2.5 mm SWNT from microwave plasma CVD; T-MWNT, 400 μm MWNT from thermal CVD; F-MWNT, 2 mm MWNT from floating CVD; and water, water concentration inside $30 \mu\text{m}$ SWNT from ACCVD. (b) Relationship of the CNT array height and the effective feedstock concentration at the array root, predicting the critical height above which these various CNT arrays will meet the strong diffusion resistance.

TABLE 1: System Parameters and As-Calculated φ and η

parameters	abb.	unit	A-SWNT	S-SWNT	P-SWNT	T-MWNT	F-MWNT
temperature	T	(K)	1073	1023	873	1023	1073
molecular weight	M	(-)	46	28	16	28	84
density	-	(g/cm ³)	0.041	0.037	0.067	0.014	0.082
CNT diameter	-	(nm)	2	3	2	10	29
number density	-	(μm^{-2})	8500	5200	14000	300	21
porosity	ρ	(-)	0.973	0.963	0.956	0.976	0.986
inter-tube distance	-	(nm)	8.8	10.9	6.5	48	189
mean free path	λ	(nm)	16000	206	5500	196	91
growth rate	-	($\mu\text{m/s}$)	0.2	3.75	0.05	1.2	0.5
reaction constant	k_s	(mm/s)	2.4	9.2	5.7	0.12	0.35
diffusion coefficient	D_e	(mm ² /s)	1.3	2.0	1.5	8.5	16.9
length	L	(mm)	0.03	2.5	2.5	0.4	2
proposed number	φ	(-)	0.054	11.3	9.7	0.0057	0.042
effective factor	η	(-)	0.949	0.081	0.093	0.994	0.960

to determine φ , and thus the degree of diffusion difficulty, have quite large difference among various CVD processes, especially between SWNT and MWNT arrays. D_e in SWNTs is usually 1 order of magnitude lower than that in MWNT because SWNTs are much more densely packed than MWNT (the intertube distance is smaller). Reaction constants are obtained experimentally from equation $r = k_s SC$. Larger k_s for SWNT growth is due to the lower carbon source concentration (C) but similar CNT growth rate (r). One possible physical reason for this difference in growth constant might be the higher catalytic activity for smaller metal particles in absorbing and decomposing hydrocarbon molecules. Because of these differences, it is suggested that, for millimeter scale SWNTs, φ is usually much larger than 1, and even if there is no catalyst poisoning, the growth rate of millimeter scale SWNT arrays will still drop to only 10% because of the strong feedstock diffusion resistance. However, as the concentration at the root of array is of little difference from the bulk concentration, above 90%, even when there is no catalyst deactivation (if considering a decrease of k_s in real systems, the concentration would be higher), the diffusion resistance seems to not be the dominant reason for the decreasing growth in MWNT arrays. The feedstock concentration distribution in these CNT arrays is presented in Figure 2a. As the φ is simply L dependent, we can also predict the critical length, as shown in Figure 2b, above which diffusion problem begins to take an effect. It seems that we might not need to worry about diffusion resistance for MWNTs before we can grow almost 10 cm to 1 m high CNT arrays, unless the diffusion phenomenon inside a CNT array is much different from classic Knudsen theory.

From eq 6, the influences of different parameters on the diffusion behavior can be investigated, and strategies to overcome the diffusion limit for the SWNT growth can also be revealed. Increasing D_e and decreasing k_s or L are all possible ways to decrease φ . However, the influences of these parameters are very limited because to bring diffusion-limited processes to the reaction controlled region one usually needs to decrease φ by 2 orders of magnitude, as expressed in eq 7. One promising approach is to pattern the continuous CNT film into a pillar-like or sheet-like microstructure to allow easy side diffusion, as demonstrated by Zhong et al.²⁶ However, we found this strategy did not work for our F-MWNT in yielding longer CNT arrays.³⁰ This means there exists strong diffusion resistance in P-SWNT but not in F-MWNT, which agrees well with the above calculated results on these two situations. One may also notice the edge of the CNT arrays produced by the “super growth” method is usually higher than the center part of the array. This might also be evidence for the diffusion limit in this process. Besides Zhong’s strategy, gradually increasing the feedstock partial pressure during the growth so as to keep the

effective concentration at the CNT root constant might be another way to overcome this diffusion limit caused growth decay.

As to the error in this calculation, it is unavoidable since the influences of some factors, for example, the bundle structure of SWNTs, the conversion rate of feedstock to CNT, tortuosity of diffusion channel (we assume it to be 1.5 in all cases), are simplified or excluded in the above discussions. However, as mentioned above, error within 1 order of magnitude in estimate of φ will not lead to a significant difference in concluding the extent of the diffusion limit. As the largest error lies on the calculation of D_e , further work on direct measurement of D_e is undergoing. Nevertheless, φ is helpful in understanding the role of growth parameters on the diffusion limit and the different diffusion behaviors inside SWNT and MWNT arrays.

To conclude, here, we present a versatile model for one-dimensional diffusion during the root growth of aligned CNT arrays. The proposed nondimensional modulus can be used to quantitatively evaluate the degree of the diffusion limit of feedstock, as well as byproduct molecules. The results show that, for millimeter scale SWNT arrays, the feedstock concentration at the root of the array is much lower than the bulk concentration, while for millimeter scale MWNTs the decreasing growth cannot be attributed to a diffusion limit. The results generated from the model agree well with experiment data. Possible strategies to grow longer CNTs in those diffusion-limited processes can be revealed.

Acknowledgment. This work was partially supported by FANEDD (No. 200548), NSFC program or key program (No. 20606020, No. 20736004, No. 20736007), China National Program (No. 2006CB932702), Key Project of Chinese Ministry of Education (No. 106011), Grant-in-Aid for Scientific Research (No. 19206024 and No. 19054003) from the Japan Society for the Promotion of Science, and SCOPE (No. 051403009) from the Ministry of Internal Affairs and Communications.

Supporting Information Available: Growth curves of aligned SWNT arrays from alcohol CVD and aligned MWNT arrays from floating CVD (Figure S1), evidence for the first-order reaction from ethanol to CNT in alcohol CVD (Figure S2), further explanation of eq 5, details of the calculation, and some additional discussion. This material is available free of charge via the Internet at <http://pubs.acs.org>.

References and Notes

- (1) Li, W. Z.; Xie, S. S.; Qian, L. X.; Chang, B. H.; Zou, B. S.; Zhou, W. Y.; Zhao, R. A.; Wang, G. *Science* **1996**, *274*, 1701.

- (2) Rao, C. N. R.; Sen, R.; Satishkumar, B. C.; Govindaraj, A. *Chem. Commun.* **1998**, 1525.
- (3) Ren, Z. F.; Huang, Z. P.; Xu, J. W.; Wang, J. H.; Bush, P.; Siegal, M. P.; Provencio, P. N. *Science* **1998**, *282*, 1105.
- (4) Fan, S. S.; Chapline, M. G.; Franklin, N. R.; Tomblor, T. W.; Cassell, A. M.; Dai, H. J. *Science* **1999**, *283*, 512.
- (5) Murakami, Y.; Chiashi, S.; Miyauchi, Y.; Hu, M. H.; Ogura, M.; Okubo, T.; Maruyama, S. *Chem. Phys. Lett.* **2004**, *385*, 298.
- (6) Hata, K.; Futaba, D. N.; Mizuno, K.; Namai, T.; Yumura, M.; Iijima, S. *Science* **2004**, *306*, 1362.
- (7) Zhong, G. F.; Iwasaki, T.; Honda, K.; Furukawa, Y.; Ohdomari, I.; Kawarada, H. *Chem. Vapor Depos.* **2005**, *11*, 127.
- (8) Liu, K.; Jiang, K. L.; Feng, C.; Chen, Z.; Fan, S. S. *Carbon* **2005**, *43*, 2850.
- (9) Li, X. S.; Cao, A. Y.; Jung, Y. J.; Vajtai, R.; Ajayan, P. M. *Nano Lett.* **2005**, *5*, 1997.
- (10) Pinault, M.; Pichot, V.; Khodja, H.; Launois, P.; Reynaud, C.; Mayne-L'Hermite, M. *Nano Lett.* **2005**, *5*, 2394.
- (11) Zhu, L. B.; Xiu, Y. H.; Hess, D. W.; Wong, C. P. *Nano Lett.* **2005**, *5*, 2641.
- (12) Iwasaki, T.; Zhong, G. F.; Aikawa, T.; Yoshida, T.; Kawarada, H. *J. Phys. Chem. B* **2005**, *109*, 19556.
- (13) Xiang, R.; Zhang, Z. Y.; Ogura, K.; Okawa, J.; Einarsson, E.; Miyauchi, Y.; Shiomi, J.; Maruyama, S. *Jpn. J. Appl. Phys.* **2008**, in press.
- (14) Zhu, L. B.; Hess, D. W.; Wong, C. P.; *J. Phys. Chem. B* **2006**, *110*, 5445.
- (15) Hart, A. J.; Laake, L. V.; Slocum, A. H. *Small* **2007**, *3*, 772.
- (16) Maruyama, S.; Kojima, R.; Miyauchi, Y.; Chiashi, S.; Kohno, M. *Chem. Phys. Lett.* **2002**, *360*, 229.
- (17) Maruyama, S.; Einarsson, E.; Murakami, Y.; Edamura, T. *Chem. Phys. Lett.* **2005**, *403*, 320.
- (18) Murakami, Y.; Maruyama, S. *Chem. Phys. Lett.* **2006**, *422*, 575.
- (19) Einarsson, E.; Murakami, Y.; Kadowaki, M.; Maruyama, S. *Carbon* **2008**, in press.
- (20) Einarsson, E.; Kadowaki, M.; Ogura, K.; Okawa, J.; Xiang, R.; Zhang, Z. Y.; Yamamoto, T.; Ikuhara, Y.; Maruyama, S. *J. Nanosci. Nanotechnol.* **2008**, in press.
- (21) Murakami, Y.; Miyauchi, Y.; Chiashi, S.; Maruyama, S. *Chem. Phys. Lett.* **2003**, *377*, 49.
- (22) Xiang, R.; Luo, G. H.; Qian, W. Z.; Zhang, Q.; Wang, Y.; Wei, F.; Li, Q.; Cao, A. Y. *Adv. Mater.* **2007**, *19*, 2360.
- (23) Levenspiel, O. *Chemical Reaction Engineering*, 2nd ed.; Wiley-VCH: Weinheim, Germany, 1972.
- (24) Futaba, D. N.; Hata, K.; Yamada, T.; Mizuno, K.; Yumura, M.; Iijima, S. *Phys. Rev. Lett.* **2005**, *95*.
- (25) Deal, B. E.; Grove, A. S. *J. Appl. Phys.* **1965**, *36*, 3770.
- (26) Zhong, G. F.; Iwasaki, T.; Robertson, J.; Kawarada, H. *J. Phys. Chem. B* **2007**, *111*, 1907.
- (27) Zhou, W. P.; Wu, Y. L.; Wei, F.; Luo, G. H.; Qian, W. Z. *Polymer* **2005**, *46*, 12689.
- (28) Zhang, G. Y.; Mann, D.; Zhang, L.; Javey, A.; Li, Y. M.; Yenilmez, E.; Wang, Q.; McVittie, J. P.; Nishi, Y.; Gibbons, J.; Dai, H. J. *Proc. Natl. Acad. Sci. U.S.A.* **2005**, *102*, 16141.
- (29) Xiang, R.; Luo, G. H.; Qian, W. Z.; Wang, Y.; Wei, F.; Li, Q. *Chem. Vapor Depos.* **2007**, *13*, 533.
- (30) Xiang, R.; Luo, G. H.; Yang, Z.; Zhang, Q.; Qian, W. Z.; Wei, F. *Nanotechnology* **2007**, *18*, 415703.
- (31) Zhang, Q.; Zhou, W. P.; Qian, W. Z.; Xiang, R.; Huang, J. Q.; Wang, D. Z.; Wei, F. *J. Phys. Chem. C* **2007**, *111*, 14638.
- (32) Futaba, D. N.; Hata, K.; Namai, T.; Yamada, T.; Mizuno, K.; Hayamizu, Y.; Yumura, M.; Iijima, S. *J. Phys. Chem. B* **2006**, *110*, 8035.
- (33) Zhong, G. F.; Iwasaki, T.; Kawarada, H. *Carbon* **2006**, *44*, 2009.
- (34) Zhu, L. B.; Xiu, Y. H.; Hess, D. W.; Wong, C. P. *Nano Lett.* **2005**, *5*, 2641.